

# UNIQUE METHODS OF ENHANCING ENGINEERING PROPERTIES OF GEOMATERIALS FOR SLOPES, EMBANKMENTS AND PAVEMENT STRUCTURES

J Mukabi<sup>1</sup>, K Gono<sup>2</sup>, R Hatakeyama<sup>3</sup>, Abiy Tesfaye<sup>4</sup>

<sup>1</sup>Katahira & Engineers International, Kenya, drmukabi@katahira.com

<sup>2</sup>Kajima Corporation, Addis Ababa, Vietnam

<sup>3</sup>Kajima Corporation, Addis Ababa, Ethiopia

<sup>4</sup>European Union, Addis Ababa, Ethiopia

## ABSTRACT:

The use of geomaterials for road construction and geotechnical structures is a definite prerequisite. However, in most cases, geomaterials are usually deficient or lacking in several of the properties necessary for their use as engineering materials. Such cases are aggravated when the engineer encounters problematic soils, which are normally susceptible to even the slightest of changes in environmental factors such as moisture-suction variations. Moreover, when such materials are adopted for engineering purposes, the roads and geotechnical structures have a tendency of either deteriorating at an alarming rate and/or failing altogether. In this study, innovative experimental methods and recently derived powerful analytical tools have been employed to develop several unique methods of enhancing the engineering properties of geomaterials. This paper essentially describes the foregoing and discusses the design and construction of such methods as Consolidation and Shear Stress (CSSR), Optimum Mechanical and Chemical (OPMC) Stabilization, SS (Suction-Stress), MCI (Moisture Control Interface) and Rerap (Replacement and Rapping), developed in this study, for purposes of enhancing geomaterial and structural engineering properties. The study concludes that the methods developed are effective in enhancing engineering properties, whereas the proposed analytical tools can be quite useful in not only evaluating post-construction structural and serviceability levels, but also determining vital parameters and inputs for numerical modelling and prediction for future design and construction.

## 1. INTRODUCTION

### 1.1. Background

In their natural state most geomaterials are usually deficient in one or more of the particle fractions required. Long term consolidation, mechanical and chemical stabilization, reinforcement by use of such methods as the geotextiles and/or Tensar Geogrids, for example, are techniques applied in enhancing the engineering properties and performance of geomaterials. The main objective of so doing is to achieve a pavement or geotechnical engineering structure which, under loading conditions, is appreciably resistant to compression and lateral displacement. In general, for geotechnical engineering structures, such composite layers that constitute the structure are considered such that the compounded effects of consolidation, compaction and particle size distribution tend towards a correctly proportioned ratio that would yield optimum density and adequate strength to resist stress-induced deformation. Jardine and Potts (1988), Aoki et al. (1990), Tatsuoka and Kohata (1994), Whittle and Hashash (1994), Mukabi (1995b), Mukabi (2001a) and Mukabi and Shimizu (2001b) have demonstrated this phenomenon in detail, whereby Mukabi and Shimizu (2001b) further showed that geomaterial which is mechanically stabilized at a ratio tending towards an optimum value may contribute greatly to preventing, to an appreciable extent, the intrusion of subgrade material to upper

layers. The detrimental effect of such intrusion on the mechanical stability of pavement layers can be observed from the results presented in this paper.

Given the importance of enhancing the properties and performance of geomaterials, Mukabi (2001a) proposed a pragmatic method of determining an Optimum Batching Ratio for more precise and enhanced mechanical stabilization.

The necessity to develop this method prevailed when, in late 1997 to early 1998, the El-Nino floods caused colossal damage to the tune of approximately US\$ 36 million on the pavement structure of the Tana Basin Road Project constructed under the Tana Basin Road Flood Recovery and Rehabilitation Project (ref. to Report to OECF Appraisal Mission for The Additional Loan to Tana Basin Road Project in the Republic of Kenya, March 1999). As a result of this damage, the loan Project funded by OECF (currently known as the Japan Bank of International Cooperation, JBIC) was faced with vast geotechnical problems that would require additional funding of at least 40%. As a consequence of the problems, the Tana Basin Road Project Technical Committee embarked on a research to enhance the mechanical properties of the available geomaterials based on some ideas that had been proposed by Mukabi et al., (1997). The successful implementation of the proposed mechanical stabilization design method would realize cost savings of up to 40% on the hydraulic structures and about 55% on the method of construction [(ref. to (1) Hydrological Review and Analyses for Hydraulic Design of Bridge and Major Culvert Structures and Determination of Areas of Protection Volumes I and II. May, 2000, (2) Engineering Report on the Design and Construction of Reinforced Earth Embankments (The Terre Armee Method) July, 2000; CPC Reports on the Tana Basin Road Project Phase II].

## **1.2. Preamble on Advantage of Application of The Newly Developed Techniques**

In this study, innovative experimental methods and recently derived powerful analytical tools have been employed to develop several unique methods of enhancing the engineering properties of such geomaterials. Experimental and testing methods such as Triaxial, Unconfined Compression (UCS), California Bearing Ratio (CBR), Rebound Deflection (RD), Point and Plate Loading Tests (PLT), were innovatively modified for mainly determining and characterizing as precisely as possible, the physical, mechanical, strength, bearing capacity, durability and deformation properties of geomaterials usually used in the construction of civil and geotechnical engineering structures.

On the other hand, analytical techniques developed on the basis of hi-tech experimental methods have been tailored for purposes of uniquely evaluating the influence of environmental factors on geomaterials and structures as well as establishing the rates and levels of their deterioration with time. This paper essentially describes the foregoing and specifically discusses the design and construction of road pavement structures based on such methods as Long-term Consolidation (Staging Construction), OPMC Stabilization, Suction-Stress, Moisture and Swell Control Interface and Rerap, developed in this study, for purposes of enhancing geomaterial and structural engineering properties. The effective application of these methods in Value Engineering terms i.e., cost vs. structural soundness, is demonstrated through Case Study Analysis of the performance of some roads and geotechnical structures already constructed in the East African region.

The study concludes that the methods developed are effective in enhancing engineering properties, whereas the proposed analytical tools can be quite useful in not only evaluating post-construction structural and serviceability levels, but also determining vital parameters and inputs for numerical modelling and prediction for future design and construction. The

paper also depicts how such data and information can be applied to achieve effective management of road infrastructure assets substantially in terms of the design and implementation of suitable and appropriate maintenance policies, techniques and systematic prioritization of works.

## 2. EXAMPLE OF SUSCEPTIBILITY OF GEOMATERIALS AT NORMAL AND CRITICAL STATE CONDITIONS

### 2.1. Influence of Moisture~Suction Variations

The change in the moisture regime of any clayey geomaterial body has been known to highly impact on the strength and deformation resistance of the particular materials. Figure 1 to 5 clearly demonstrate the importance of taking this factor into account during design and construction Quality Control (QC).

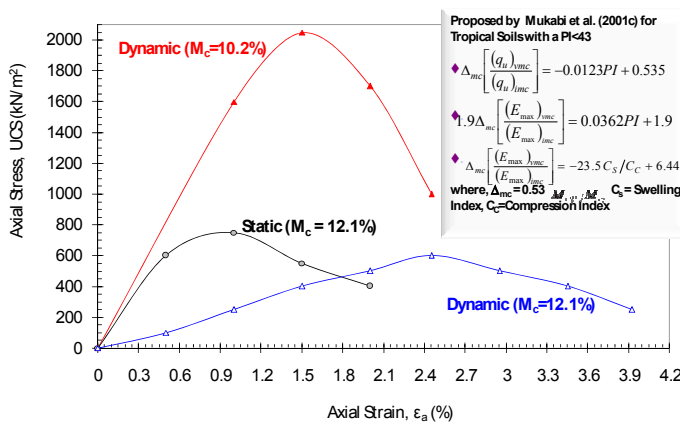


Figure 1 – Moisture-suction variation

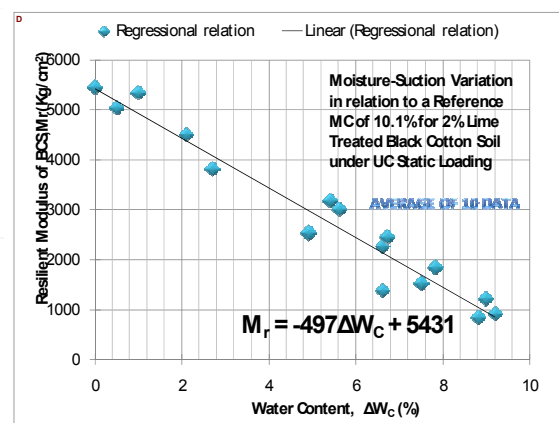


Figure 2 – Effect on resilient modulus

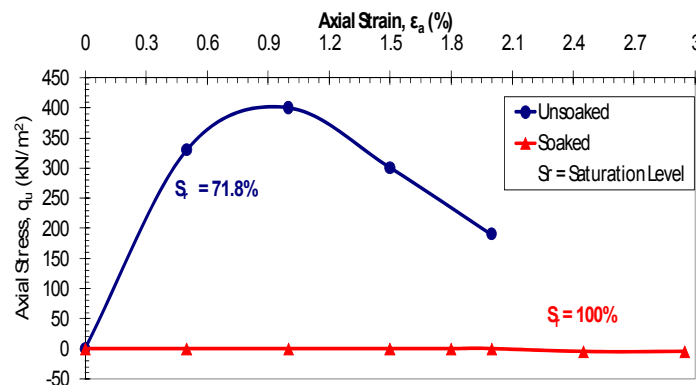


Figure 3 – Detrimental effect of soaking

Figure 1 is a typical depiction of the effect of moisture~suction variation on statically and dynamically loaded tropical soils, whereas Figure 2 shows the same effect on the resilient modulus (deformation resistance) of lime treated Black Cotton (expansive) Soil. On the other hand, Figure 3 demonstrates the detrimental effect of soaking geomaterials under Critical State conditions. Figure 4 and 5 are a clear nomographic indication of the significant impact of moisture~suction variation in relation to varying material quality. The inset equations also indicate that the moduli of deformation or deformation resistance is susceptible to moisture~suction variations, a fact that has also been derived from Figure 26 and 27. The figures were used in deriving various design parameters. For example, the bearing strength and deformation resistance parameters were determined from field tests

carried out on the natural sandy clay of the Sudd Flood Plain in Jalle, Southern Sudan, which is the location of the White Nile Oil Exploration activities and more so the site of the drilling pad foundations, and various other sites for pavement structures and bridge foundation design in eastern Africa. The moisture contents were then arbitrarily varied to simulate varying moisture~suction conditions mainly precipitated by seasonal effects and subsurface water action or underground water seepage.

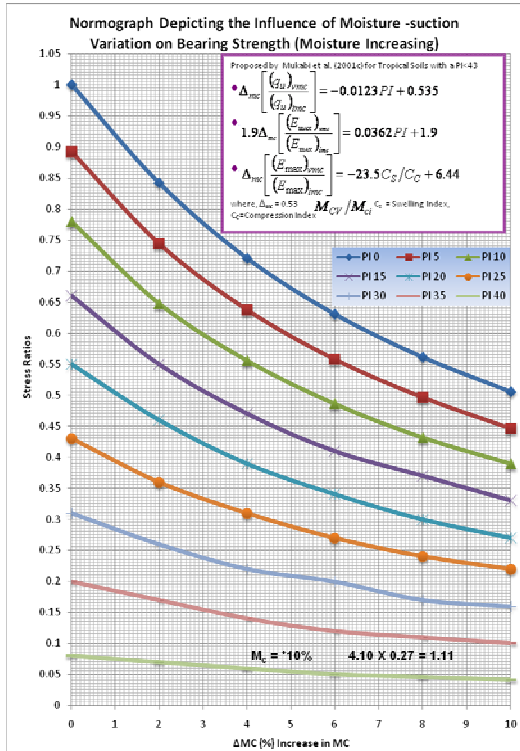


Figure 4 - Normograph (Moisture Increasing)

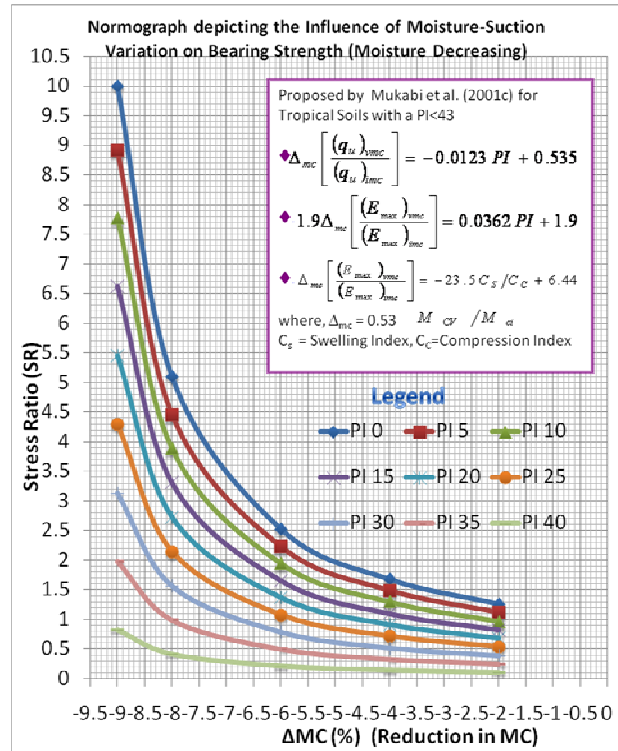


Figure 5 - Normograph (Moisture Decreasing)

## 2.2. Influence of Inferior Material Intrusion

One of the critical phenomena that has never quite been considered by researchers and practicing Engineers is the crucial detrimental effect of Intrusion of native subgrade material into the overlying layers of the pavement, which usually results in the ultimate degradation of the layers Mukabi (2001a). Depending on the nature of the subgrade, topography of environment and seasonal changes, intrusion of native subgrade material into overlying layers of the pavement structure, as depicted in Figure 6, can be rampant and extremely detrimental.



Figure 6 – Material intrusion

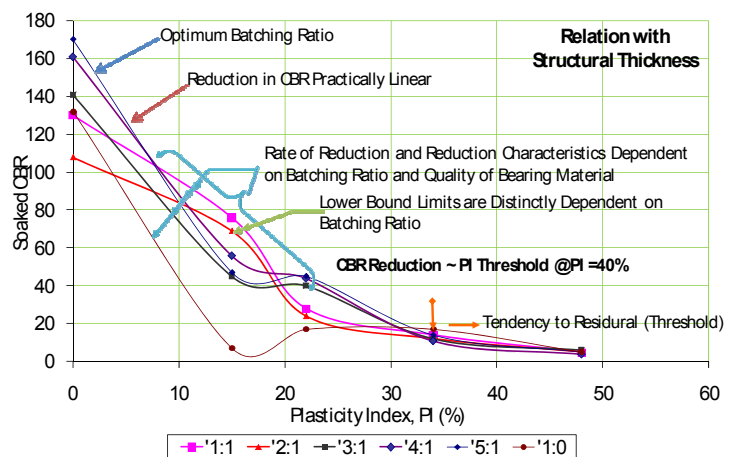


Figure 7 – Effect on bearing strength

The consequences of such a physical action are the deterioration of bearing capacity, cohesion intercept ( $c$ ) and internal friction ( $\phi$ ) as well as mechanical stability. Some of the results of the quantitative analysis of this factor are presented in Figure 7 and further discussed for expansive soils in Mukabi and Gono (2007f, This Conference) and Mukabi et al. (2003c). In this series of experimental testing, materials with varying qualities and properties were infiltrated into high quality crushed aggregate base course material mechanically stabilized at varying ratios (0~40mm:0~5mm aggregate). Figure 7 clearly indicates that: 1) inferior material intrusion into the upper layers drastically reduces the bearing strength. 2) The magnitude and rate of reduction in bearing capacity is a direct function of the quality of material and batching ratio. 3) The threshold of the CBR reduction is at approximately PI=35%. 4) The effect of subgrade material intrusion ceases after the PI reaches the threshold value. The results indicate therefore, that it is imperative to take this fact into consideration during the structural design of a pavement.

### 2.3. Typical Problematic Tropical Soils in Eastern Africa

The typical expansive and problematic soils in the eastern Africa region are mainly represented by Black cotton soils, which are usually tropical clays which are essentially products of physical and chemical in-situ weathering of igneous, sedimentary and metamorphic rocks under varying environmental conditions. The formation of these soils is highly influenced by a complex interaction of various variables, such as weathering, erosion and climatic changes as well as type of original parent rock, local topography, drainage and cycle factors which strongly influence their engineering behaviour. As a consequence, their characterization for use as suitable engineering materials becomes extremely complex since they are highly susceptible to various environmental changes.

These clays typically occur in flat, poorly drained areas with annual average precipitation levels of between 500~1250mm and altitudes of 1~2000m underlain by lava and tuffs. Typical grading characteristics of a representative black cotton soil would be 60% clay, 30% silt and 10% sand. Table 1 presents some typical properties while a global classification of these soils is given in Table 2.

Table 1 - Typical Properties of Black Cotton Soil

Property	Value
Liquid Limit LL (%)	37~83
Plasticity Index PI (%)	16~45
Moisture Content $w$ (%)	16~40
Shrinkage Limit SL (%)	8~20
Percent Passing 75 $\mu$ m	75~95
Free Swell (%)	70~165
Swelling Pressure $kN/m^2$	0~80
Linear Shrinkage (%)	18~35
Specific Gravity $G_s$	2.47~2.56
Dry Density $\gamma_d$ $kg/m^3$	1920~2050

Table 2 - Classification of Black Cotton Soil

Soil Parameter	Classification		
	Moderate Swellability	High Swellability	Very high Swellability
Dry Density $\gamma_d$	$<15kN/m^3$	$15 \leq \gamma_d \leq 16$	$>16$
Clay content $C < 0.002$	$<40\%$	$40 \leq c \leq 55$	$>55$
Liquid Limit (LL)	$<48\%$	$40 \leq LL \leq 55$	$>65$
Plasticity Index (PI)	$<30\%$	$30 \leq PL \leq 40$	$>40$
Shrinkage Index (IS)	$<30\%$	30~60	$>60$
Swell Pressure	$<120kN/m^2$	120~600	$>600$

These soils are also known to be highly susceptible to pore-grain moisture-suction matrices characterized mainly by swelling due to wetting and shrinkage due to drying that prompts accelerated reduction or gain in strength respectively. This characteristic is mainly

attributed to the excessively large surface areas and alteration of clay minerals on dehydration and aggregation of fine particles that form larger particles due to the presence of cementing agents and/or pore fluid characteristics usually found to be permanent. The resulting effect is the formation of increased suction pressures. Changes in the plasticity characteristics of these soils are known to be influenced by the wetting and drying historical hysteresis (ref. to Figure 8), whereby the changes are less significant for the clays which are subjected to conditions that are conducive to alternate drying and wetting over a geological time scale (ref. Pandian et al, 1993, Mukabi, 1998). In dealing with such expansive clays it is necessary to investigate both the quantitative and qualitative influence of such aspects on the microstructure and mechanical properties which are dependent on the pore geometry. This can give an insight of suitable engineering applications that can effectively control the moisture-suction states to quasi-equilibrium states.

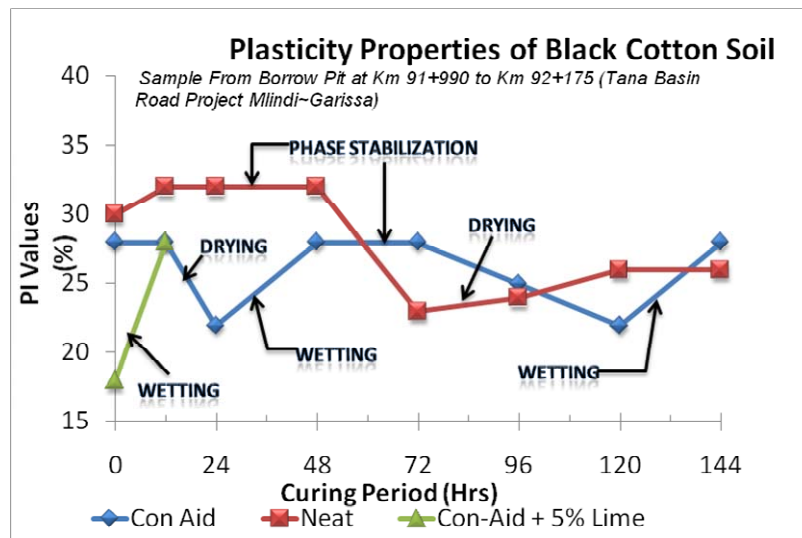


Figure 8 – Black Cotton Soil plasticity

When designing for, and adopting such expansive soils during road construction, serious care must be taken to cater for such environmental factors which can have extremely serious impacts on the foundations of civil engineering structures.

### 3. PRAGMATIC METHODS OF ENHANCING GEOMATERIAL ENGINEERING PROPERTIES

#### 3.1. Example of Innovative Method of NDT Testing

##### 3.1.1. Theoretical Considerations

The practical use of non-destructive deflection testing has been an integral part of the structural evaluation and rehabilitation process for several decades. During the initial stages of its application, the total measured pavement was used as a direct indicator of structural capacity. This method was thence applied by most agencies in developing failure criteria, particularly for flexible pavements, that related the maximum deflection to the number of allowable load repetitions. While deflection criteria similar to that shown in this Figure 9 is still in common use, recent technical advances indicate that maximum rebound deflection, as an independent parameter, is not the most accurate nor applicable parameter for the variety of pavement structures encountered in practice. In normal practice, it is usually considered that pavements may be structurally distressed by either excessive deformations and/or load-associated fracture of a particular layer.

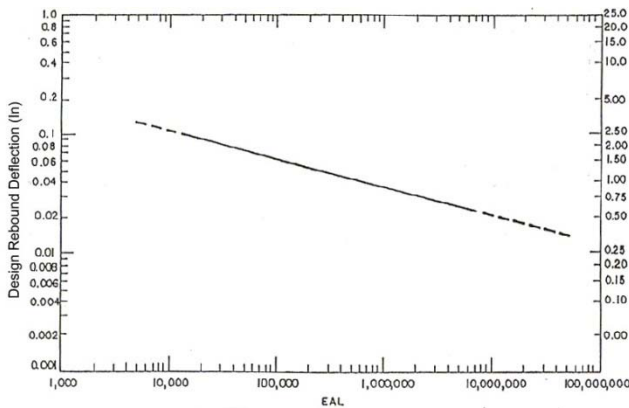


Figure 9 - Failure Criteria on Rebound Deflection

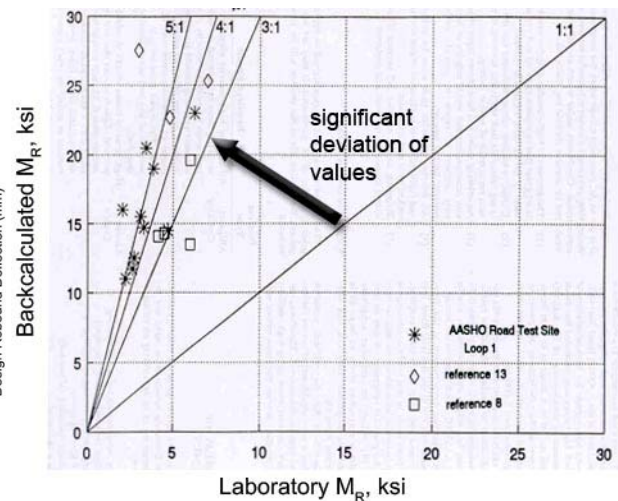


Figure 10 - Significant Deviation

Theoretically however, the maximum elastic deflection may be more indicative of the pavement's capacity to resist repetitive shear displacements leading to rutting, while the curvature radius of the pavement under load is more indicative of overall resistance to repeated load fracture of a pavement layer. As a consequence, several agencies have redefined that deflection-repetition-performance criteria to account for this very important concept. On the other hand, although the State of the Art dynamic NDT-deflection methodologies are a technical improvement over approaches that use only deflection-life performance criterion, the engineer must recognize the fact that they are neither perfect nor above any envisaged modifications as technology and application advances. Furthermore, the engineer must not blindly use NDT deflection results, but rather assess quantitatively, whether the results obtained are reasonable or not. Mukabi et al. (2003a) realized the necessity to modify innovatively, the contemporary NDT testing and analytical techniques.

Consequently, the necessity to innovate modified NDT deflection testing and analytical techniques has primarily been precipitated by two main reasons. On the one hand, both the static-creep and "dynamic" NDT deflection testing equipment and devices have numerous limitations (ref. to Figure 10), some of which include : 1) The devices usually cannot make direct measurements of the stress-strain properties of the pavement structure, hence data is predominantly obtained by inference. 2) Measurements are highly susceptible to environmental factors such as temperature moisture content as contributed by seasonal changes, wind effects, vibration effects, gradient of slopes etc. 3) The ultimate rebound is a function of various pavement components such as pavement type, structural configuration, layer interaction, relative pavement stiffness, composite pavement stiffness, surface conditions and surface layer stiffness. 4) Accurate determination of layer of measurement cannot be made directly but is usually wide inference making the data and reciprocal precision susceptible to the effects outlined in 3 above. On the other hand, and advanced analytical method of effectively applying the following fundamental principles of that deflection testing is necessary. They are: 1) multiple structural distress types including both deformation and fracture must be logically accounted for in the interpretation of deflection testing results; and 2) pavement layer material type (quality) and layer thickness must also be considered if deflection-repetition-performance curves are to be used. Modification of the existing techniques for purposes of advancing the confidence and precision levels is therefore considered imperative.

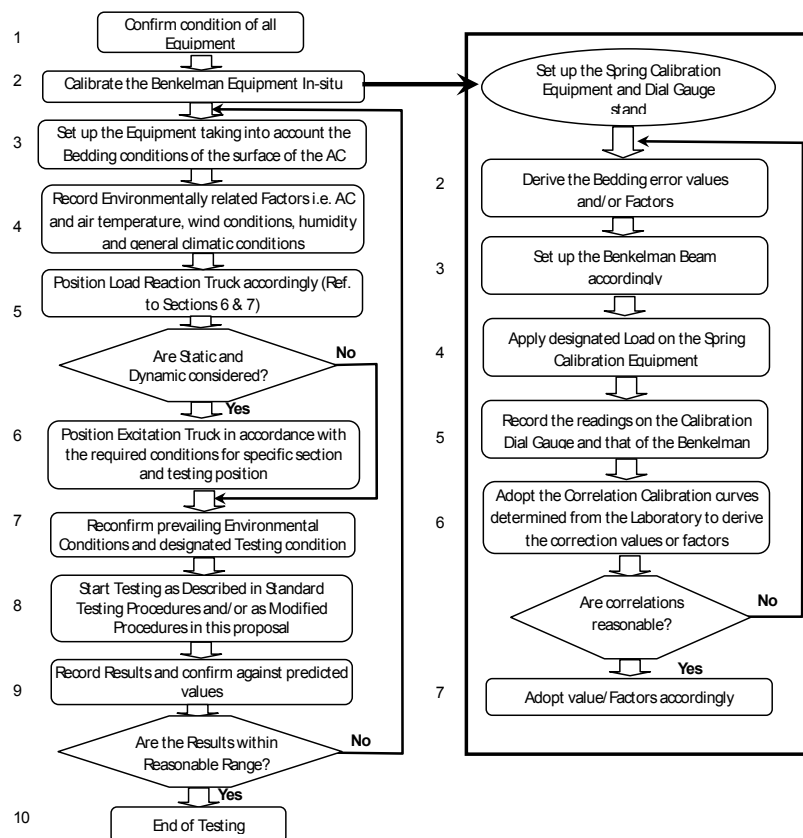
### 3.1.2. Basis and Considerations of Design of the Testing Regime

The testing programmes adopted in this Research Programme were aimed at achieving results that can form a basis for analysis oriented towards realizing the objectives stipulated under Section 3. For example, since ND small deflection testing is highly susceptible to systematic errors in measured quantities due to the correlation between its range of actual measurement and the resolution of the equipment, it was designed such that intensive calibration of the equipment be carried out in-situ under varying bedding surface, loading and environmental conditions in order to discern and isolate each unique factor that influences the measurement. To confirm the accuracy and confidence levels of these measurements, not only was a precise establishment of unit delineation and adaptation of an appropriate statistical approach taken into consideration but also augmentation with DT methods and comparative analysis with laboratory and historical data is carefully incorporated. Overall, the modified methods considered: 1) Stress-strain properties of the pavement structure. 2) Environmental factors. 3) Pavement components such as pavement type, structural configuration, layer interaction, relative pavement stiffness, surface conditions and surface layer stiffness, and, 4) Accurate determination of layer measurement.

### 3.1.3. Main Objectives of Study

The main objectives of the study therefore were: 1) Developing empirical methods of estimating modulus of elasticity and resilience. 2) Establishing appropriate models for characterizing pavement response. 3) Developing suitable methods of appropriately characterizing deflection and rebound properties. 4) Determining approximate range of dynamic load effect, and, 5) Comprehensively studying the typical pavement response in relation to various factors and aspects.

### 3.1.4. Brief Description of NDT Methods



Figures 11 Outline of Example of Innovative Newly Developed NDT Methods

Figure 11 is a brief outline of the NDT Method that was typically applied in this testing regime. Due to its propensity to cause excitation on the suspension systems of vehicles and subsequent impact on dynamic vehicle wheel loads, both short wavelength and long wavelength roughness along with other surface conditions were evaluated on the basis of in-situ measured values. Varying the points of measurement longitudinally in a systematic manner enabled the estimation of the deflection basin and area to be achieved. On the other hand, adopting scientific and engineering concepts and the application of excitation truck and vibration roller enabled the characterization of pavement response relative to stress propagation, stress distribution and stress magnitude as well as the corresponding superimposition and other effects, including confining stresses and layer interface conditions. For objectives of choice of each section, refer to Mukabi et al. (2003c).

### 3.2. Introduction of Some Aspects of Newly Developed Methods of Enhancing Engineering Properties of Geomaterials

#### 3.2.1. Application of CSSR Theories, Concepts and Practical Application

The theories and concepts introduced hereafter can be mainly adopted for: 1) Correcting laboratory tested parameters to simulate as precisely as possible, the field values and characteristics of ground foundation behaviour, 2) Design and construction quality control of staging construction of civil engineering foundations for bridges and skyscrapers, structures such as high embankments, slope stability and deep excavation as well as tunnelling in expansive and problematic soils, 3) Modelling and prediction of full-fledged field behaviour after construction of civil engineering structures and, 4) Back-calculation and analysis of settlement and deformation of civil engineering structures and, 4) Back-calculation and analysis of structures founded on geotechnical basis to facilitate foundation design and construction.

#### (1) Functions and parameters related to the concept of loading rate

Due to the importance of incorporating the analysis of the effects of loading on foundations and embankments of clayey geomaterials during modelling and design, Mukabi and Tatsuoka (1999b) developed a relation between the stress ratio at failure  $\eta_{\max}$  ( $q/p'_m$ ) and axial strain rate ( $\epsilon_a$ ) expressed in a generalized state as :

$$\eta_{\max} = A_{\eta} I_n \epsilon_a^{SR} + B_{\eta} \quad (1)$$

where constants  $A_{\eta I}$  and  $B_{\eta}$  were determined as  $A_{\eta}^A = 0.037$ ,  $B_{\eta}^A = 0.858$  and  $A_{\eta}^I = 0.043$ ,  $B_{\eta}^I = 0.76$  (Superscripts denote; A : Anisotropic; I: Isotropic; SR: Strain Rate). Based on comprehensive analysis of various clays subjected to different axial strain rates and on Equation 2 the following co-relations were derived:-

$$\omega_{SR} = A_{\eta} I_n \left( \frac{\epsilon_a^{ASR}}{\epsilon_a^{RSR}} \right) + B_{\eta} \quad (2)$$

and  $\eta_{\max}^{ASR} = \omega^{-1} \bullet \eta_{\max}^{RSR}$  (7.5) where  $\omega_{SR}$  is a strain rate function and superscripts ASR and RSR denote “Applied Strain Rate” and “Reference Strain Rate” respectively.

## (2) Functions and parameters based on SHANSEP consolidation

As was discussed by Mukabi and Tatsuoka (1999a and 1999b) and Mukabi (2001d), the “intact” specimen exhibits much more superior behaviour in comparison to the specimens reconsolidated applying the SHANSEP method. It was also derived that the higher the stress level of the consolidation stress ratio  $\eta_c=(q_c/p'_c)$ , the more the structure is destroyed through remoulding. This implies that specimens reconsolidated by applying the SHANSEP method can not be representative or correctly simulate the in-situ conditions. Consequently, correction factors have to be applied on the parameters determined adopting such a method. Based on the concepts of consolidation and shear stress ratio functions, the following correlations for  $q_{max}$ ,  $p_f$  and  $\phi_f$  were derived.

$$q_{max}^{OCS} = \frac{K_0^{NCS} \cdot q_{max}}{\left( K_0^{NCS} - \left( \frac{\eta_c^{OCS}}{\eta_c^{NCS}} \right) \cdot A \phi \cdot CSR^{NCS} \right)} \cdot \frac{\sigma_{vmax}^{OCS}}{\sigma_{vmax}^{NCS}} \quad (3)$$

$$p_f^{OCS} = \frac{K_0^{NCS} \cdot p_f^{NCS}}{\left( K_0^{NCS} - \left( \frac{\eta_c^{OCS}}{\eta_c^{NCS}} \right) \cdot A \phi \cdot CSR^{NCS} \right)} \cdot \frac{p_c^{OCS}}{p_c^{NCS}} \quad (4)$$

$$\phi_f^{OCS} = \frac{K_0^{NCS} \cdot \phi_f^{NCS}}{\left[ K_0^{NCS} - \left( \frac{\eta_c^{OCS}}{\eta_c^{NCS}} \right) \cdot A \phi \cdot CSR^{NCS} \right]} \quad (5)$$

where, subscript  $f$  denotes failure, superscript OCS and NCS denote Over Consolidated and Normally Consolidated under the SHANSEP method.

## (3) Functions and parameters related to the concept of ageing

Aging is considered to constitute mainly of two components; namely secondary consolidation associated with creep ( $\partial \varepsilon'_a / \partial t = 0$ ) and thixotropy defined as a gain in strength at constant water content. Creep is basically caused by a continuing re-arrangement of the soil particles after the overburden pressure is fully supported by the soil skeleton, whereby the excess pore pressure has dissipated. Kuhn and Mitchell (1993) proposed that creep deformation is due to sliding between particles and that although the sliding is thought to occur at solid contacts, it is visco-frictional in nature and the sliding velocity at each contact depends on the ratio of tangential to normal components of contact force. Whether the creep strains in triaxial tests accelerate or not depends principally on the magnitude of the deviator stress compared to the strength or compressibility of the sample. Mitchell (1976) proposed the following general creep equation:

$$\frac{d\varepsilon_a}{dt} = A e^{\alpha R} (t_r / t)^m \quad (6)$$

where  $R=q^t/q^f$  delineates the deviator stress level,  $t_r$  is a reference time and  $A$  and  $\alpha$  are solid constant parameters. When  $m=1$  the strain rate continues to decrease with time, while the strain rate accelerates towards failure when  $m<1$ . Considering  $m=1$  and integrating Eq. 7.9 with  $\varepsilon_a = \varepsilon_{a\alpha}$  at  $t = 1$  then,

$$\left( \varepsilon_a - \varepsilon_{a\alpha} \right) = A e^{\alpha R} l_n t \quad (7)$$

is obtained. This is similar to the expression,

$$\Delta\varepsilon_a = C_\alpha l_n(t/t_0) \quad (8)$$

representative of a one dimensional creep. Mukabi (1995), Mukabi and Tatsuoka, (1999a) reported results on the effects of aging in reconsolidation on deformation characteristics of various natural clays. The comprehensive research showed that time plays an important role in the stress-strain time history of clays. Based on comprehensive analysis of such results and considering that creep, which is predominantly associated with secondary consolidation, contributes more significantly to the strength development of clay in comparison to thixotropy and further assuming that  $\Delta\varepsilon_a$  is purely a function of consolidation properties, then the following generalized relations were derived.

$$q_{\max}^{LTC} = \frac{K_0^{STC} \cdot q_{\max}^{STC}}{\left[ K_0^{STC} - (l_n t/t_0) A\phi' \cdot CSR^{STC} \right]} \quad (9)$$

while,

$$p_f^{LTC} = \frac{K_0^{STC} \cdot p_f^{STC}}{\left[ K_0^{STC} - (l_n t/t_0) A\phi' \cdot CSR^{STC} \right]} \cdot \frac{q_{\max}^{LTC}}{q_{\max}^{STC}} \quad (10)$$

and

$$\phi_f^{LTC} = \left[ \frac{K_0^{STC}}{K_0^{STC} - (\Delta\varepsilon_a/\Delta t)_{fc}^{STC} (l_n t/t_0) \cdot A\phi' \cdot CSR^{STC}} \right] \quad (11)$$

where superscript LTC and STC denote long term and short term consolidation respectively whereas  $t$ : LTC time and  $t_0$ : STC time., for OC conditions  $(\Delta\varepsilon_a/\Delta t)_{fc}^{STC}=1$

#### (4) Functions and parameters of reconstituted clays

The adverse effects of reconstitution of clays was briefly discussed in the preceding section 7.3.2 of this paper. From the analysis of various data based on the concepts of consolidation and shear stress ratio, the following correlations that can be useful in computing  $q_{\max}$ ,  $p_f'$  and  $\phi_f'$  from CUTC tests on reconstituted clays were derived.

$$\left( \frac{q}{p_e} \right)_{\max}^I = \frac{\mu_e^R \cdot \eta_c \cdot (q/p_e)_f^R}{\left( K_{cf}^R - (\mu_e^R \cdot A\phi \cdot CSR^R) \right)} \quad (12)$$

$$\left( \frac{q}{p_e} \right)^I = \frac{\mu_e^R \cdot \eta_c \cdot (p/p_e)_f^R}{\left( K_{cf}^R - (\mu_e^R \cdot A\phi \cdot CSR^R) \right)} \quad (13)$$

and

$$\phi_f^I = \frac{\mu_e^R \cdot \eta_c \cdot \phi_f^R}{\left( K_{cf}^R - (\mu_e^R \cdot A\phi \cdot CSR^R) \right) \cdot [q/p_e]_f^R} \quad (14)$$

where superscripts I and R denote “intact” and “reconstituted” respectively and  $\mu_c^R=(q/p')_f^R$ ,  $\eta_c=(q/p')_c$ , and  $K_{cf}^R = (\sigma'_r/\sigma'_a)_{ec}^R$ .

#### 3.2.2. OPMC Stabilization Techniques

The OPMC Stabilization technique was mainly developed on the basis, theories and concepts of the OBRM (Optimum Batching Ratio Method) established in 2001 (ref. to

Mukabi, 2001a, Mukabi and Shimizu, 2001b and Mukabi et al., 2007b). Some of the results that pragmatically demonstrate the effects of this method are presented in Figs. 3.1~3.15. These results show that OPMC enhances the strength, bearing capacity, deformation resistance and linear elastic range of the various geomaterials tested.

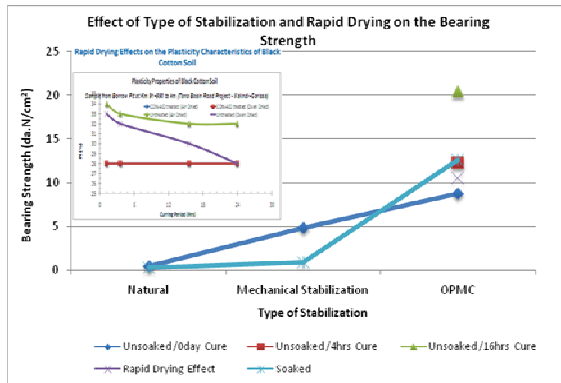


Figure 12 – Rapid drying effect

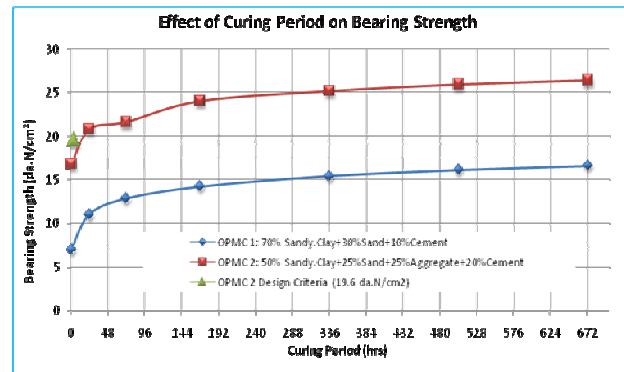


Figure 13 – Curing period effect

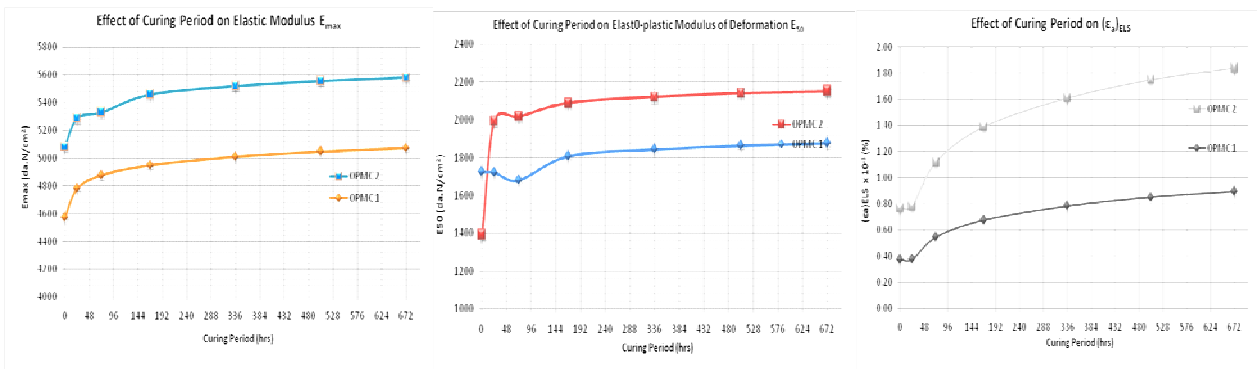


Figure 14– Curing period effect on elastic, deformation and limit strain modulus

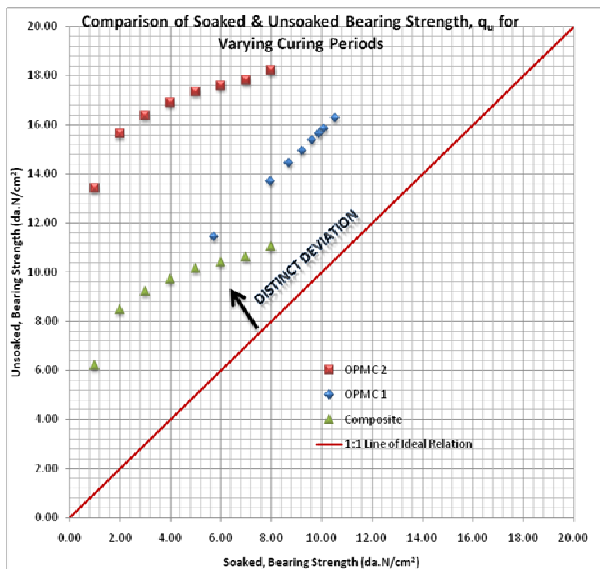


Figure 17 – Soaked vs. Unsoaked

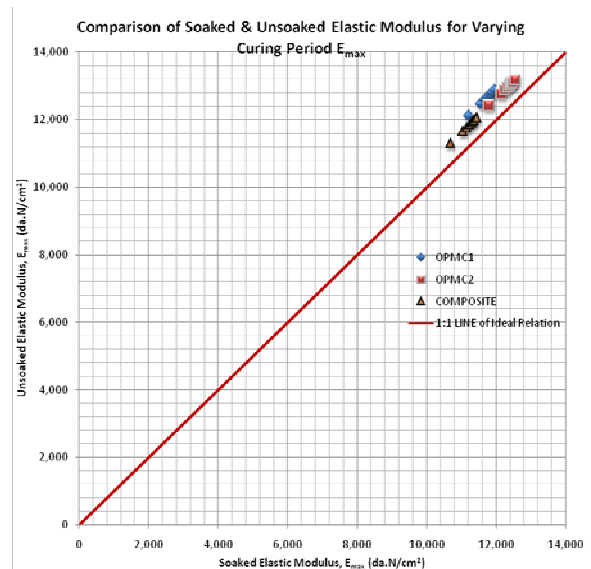


Figure 18 – Elastic modulus

### 3.2.3. Rerap Methods

*Determination of appropriate counter-measures* 1) Replacement Method - Tables 2 and 3 as well as Figures 19 and 20 show the design and QC criteria developed on the basis of research and adopted for the construction of the Addis Ababa ~ Goha Tsion Trunk Road

Project. In determining the necessary thickness  $t_{CL}$  to replace the expansive soil, the following equations proposed in this study were adopted.

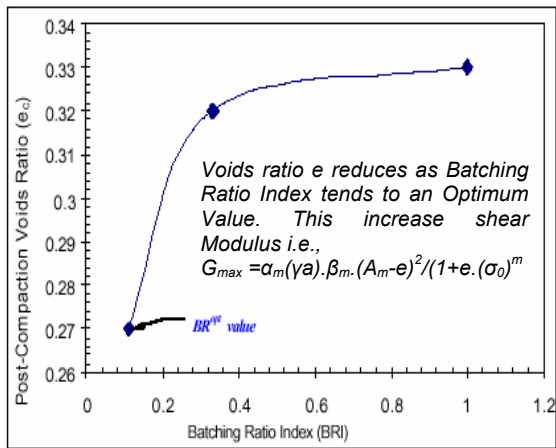


Figure 19 - BRI Vs. Voids Ratio

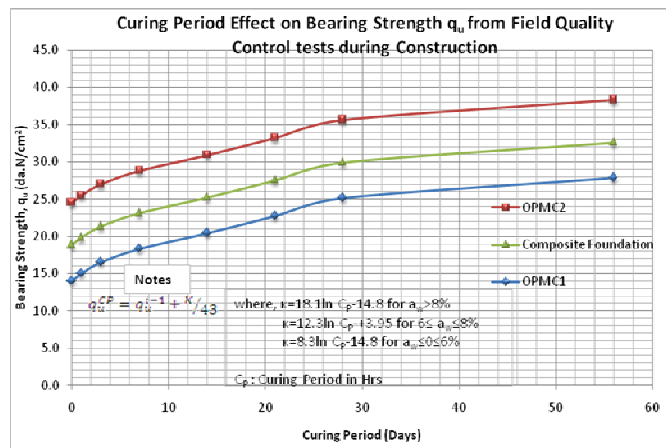


Figure 20 – Quality Control normograph

$$t_{CL} = \left\{ T_P - t_p^b \right\} \alpha S_{SP} \quad (15)$$

The total pavement thickness  $T_P$  is expressed as:

$$T_P = t_p^b \alpha R_f + t_v \quad (16)$$

And the coefficient of subgrade structural performance  $S_{SP}$  is computed from:

$$S_{SP} = \left[ e^{1/CBR_d / \alpha_e} \right]^{0.5} \quad (17)$$

On the other hand, the basic pavement thickness  $t_p^b$  from Eq. (3.10) is computed from the following equation.

$$t_p^b = \frac{\left[ A_p - B_p (\log CBR_d) + C_p (\log CBR_d)^2 \right]}{\log [N / D_p]} \quad (18)$$

Where the roughness factor  $R_f = \left[ 2R_t / (R_i - R_t) \right]^{0.25}$ :  $R_i$  is the initial roughness factor and  $R_t$  is the terminal roughness factor,  $t_v$  in Equation 11 is the positive value of the specified tolerance for pavement thickness,  $A_p=219$ ,  $B_p=211$ ,  $C_p=58$  and  $D_p=120$ . The parameter  $\alpha_e$  in Equation 12 is defined as:

$$\alpha_e = A_e e^{(B_e - C_e V_e) LL / M_{cn}} \quad (19)$$

where  $A_e=0.23$ ,  $B_e=0.54$ ,  $C_e=0.08$  are constants and  $V_e$ =Annual Average Evapotranspiration in m/year (ref. to Mukabi et al. (2003c),  $LL$ =liquid Limit in percentage and  $M_{cn}$ =Natural Moisture Content of the subgrade material expressed in percentage form. All thickness are calculated in mm. Continuous assessment and evaluation of the performance of the sections already constructed by adopting this criteria indicates that the method has so far been quite successful.

Table 3 - Determining Required Capping Layer Thickness (cm) for RE 1 Type Phase II

Coding Option	Plasticity and Swell Condition		Required Thickness for Different Subgrade Bearing Capacity				
	Plasticity Index	Swell (%) $S_m$	CBR = 1	CBR = 2	CBR = 3	CBR = 4	4<CBR<7
A	PI>45	$S_m > 10$	140	90	70	60	30
B	$35 < PI < 45$	$S_m < 10$	110	75	60	50	20
C	PI<35	$S_m < 5$	70	65	55	50	20

**Notes**

- ◆ Where the results are on the Boundary Limit or within its vicinity, the Criteria of Clay Activity ( $A_c$ ) expressed as  $A_c = 3.6R^{-2.35}$  ( $R=LL/PI$ ) may be adopted or otherwise as directed by the Consultant. For example, should the  $PI > 45$  and  $S_m < 10$ , if  $A_c < 1.0$  then option B may be adopted instead of Option A or vice versa.
- ◆ If  $A_c < 0.75$  then maximum swell values of  $S_m = 15\%$  can be allowed for Options B and C.
- ◆  $S_m$  represents maximum swell measured uniaxially after 4 days soak and under a standard surcharge pressure of 298kg/m<sup>2</sup>.
- ◆ For materials that exhibit excessively high initial rates of swell, the Consultant shall be consulted for further analysis prior to characterizing the expansive subgrade material.

Table 4 - Determining Required Capping Layer Thickness

CBR of Imported material	Required Thickness for Different Native Subgrade Bearing Capacity (cm) for RE 1 Type				Required Thickness for Different Native Subgrade Bearing Capacity (cm) RE2 Type		
	CBR = 1	CBR = 2	CBR = 3	CBR = 4	CBR = 5	CBR = 6	CBR = 7
15	70	65	55	50	40	30	20
20	60	55	45	40	30	25	20
25	55	45	40	35	25	20	15
30	50	40	35	30	20	15	10
40	45	35	30	25	15	10	10
50	40	30	25	20	10	10	10
60	35	25	20	15	10	10	10

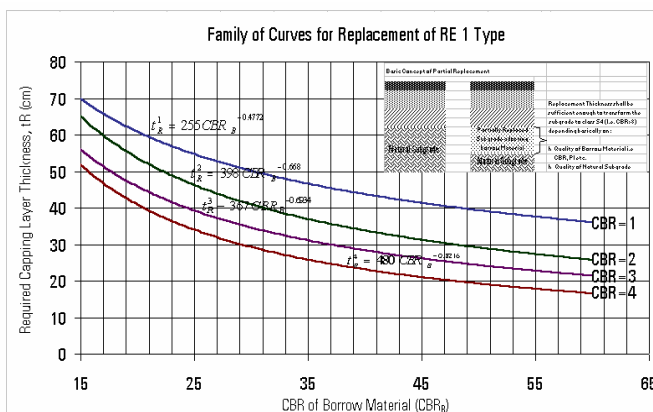


Figure 21 - Layer thickness ( $1 \leq CBR_d \leq 4$ )

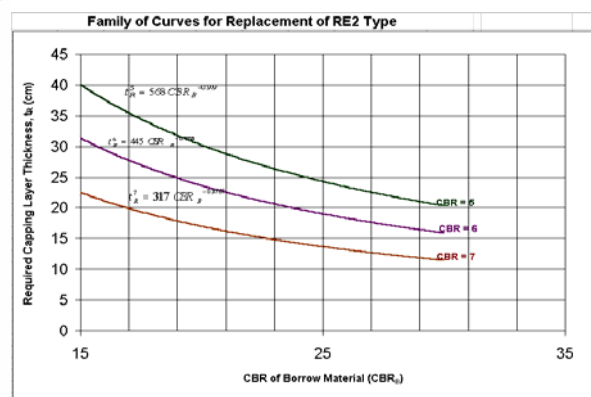


Figure 22 - ( $4 < CBR_d < 8$ )

3.2.4. MC Technique

The importance of moisture control is clearly demonstrated in Figures 4 and 5, which are nomographs that depict the influence of moisture~suction variation on the bearing strength of varying geomaterials. The variation in the nature of geomaterials is simulating through

the application of varying plasticity characteristics and magnitudes. The inset equations also indicate that the moduli of deformation or deformation resistance is susceptible to moisture-suction variations, a fact that has also been discussed in Section 4 as well as the preceding sections of this section. The on-going research on this subject intends to develop a technique of controlling the moisture content of a subgrade of an expansive nature by systematically and technically imbedding sand columns in predetermined areas or zones. Figures 23 ~ 24 present part of the preliminary results that have been obtained in the initial stages of testing. Although definite conclusions can not be derived from these results yet, the trends exhibited from these graphs are distinctly clear. In other words, imbedment of sand interface layers seems to be effective in reducing swell and increasing the bearing capacity notwithstanding the magnitude of the surcharge pressure.

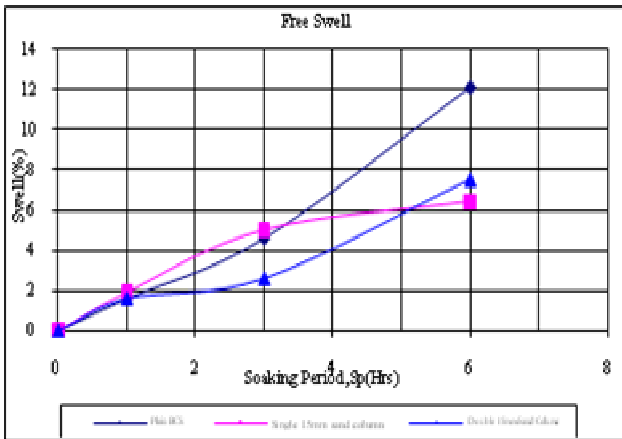


Figure 23 - Free swell soaking

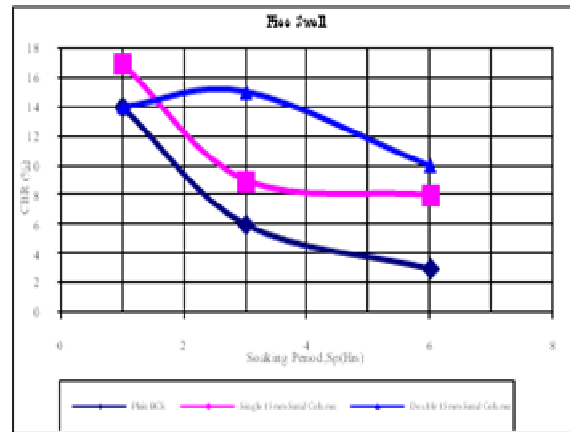


Figure 24 – Soaking period for CBR

### 3.2.5. Suction Stress Method

Research for purposes of developing this method is still in the initial stages. The basic idea is to develop a technique of constructing a subsurface drainage layer underlain by a layer compacted to a higher degree in order to induce high but varying suction stresses. The layer is intended to facilitate in directing any excess moisture away from the pavement structure. Reference can be made to section 6. of this paper which discusses maintenance and Mukabi (2004a). Figures 25 and 26 are a representation of how this technique was used by incorporating a suction stress column in the design of an OPMC Stabilized retaining wall and maintenance along the Addis Ababa ~ Debre Markos International Trunk Road, the all important northern corridor that connects Sudan and Eritrea.

Transformed Cross-section A-A for Ease of Construction

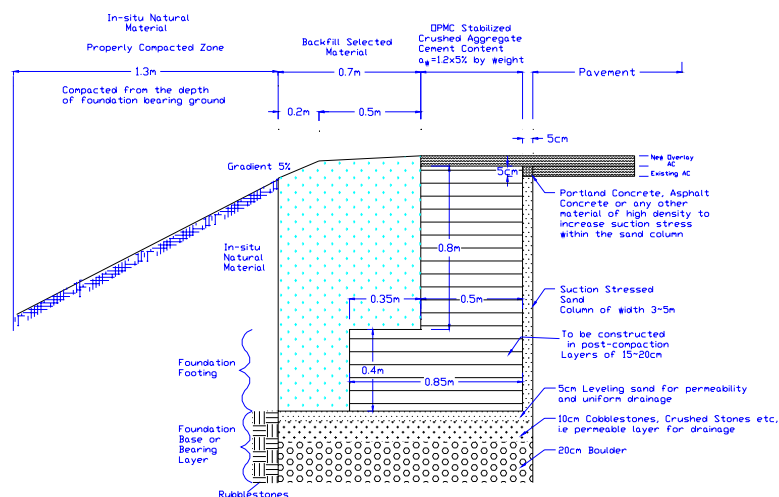


Figure 25 - Use of a Suction Column for OPMC Stabilized Retaining Wall.

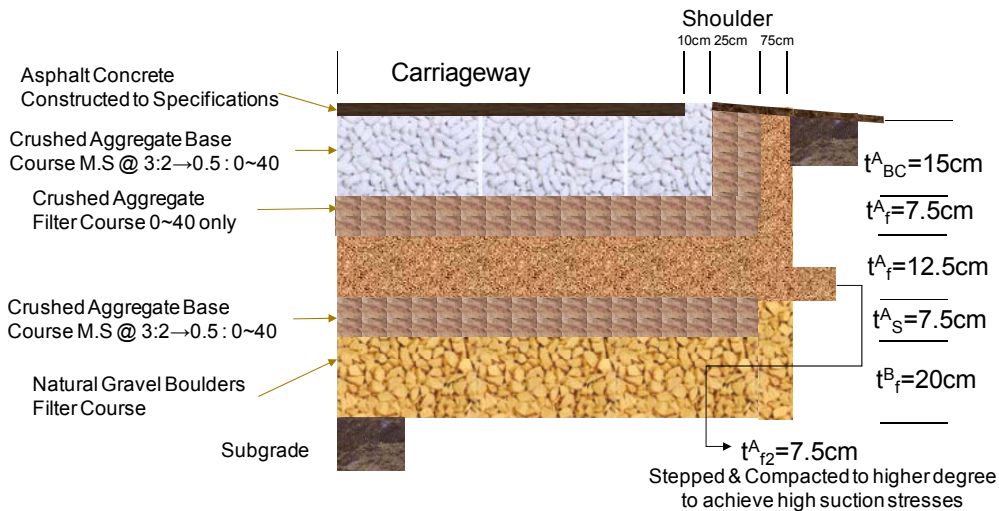


Figure 26 – Suction-stress method

### 3.2.6. Consolidation (Staging Construction) Method

#### (1) Long Term Consolidation

Mitchell (1976), Leroueil and Vaughan (1990), Mukabi (1995a), Mukabi and Tatsuoka (1999c) and Mukabi et al. (2003d) have shown that long term consolidation enhances the strength and deformation resistance of geomaterials subjected to various conditions including disturbance and swelling. Anderson and Stokoe (1978) performed resonant column tests under constant isotropic confining pressure  $\sigma'_0$ , and showed that the value of low amplitude shear modulus increases with time and expressed this empirically as depicted in the following formula.

$$G_0(t) = G_0(t-tp)[1+NG\log(t/tp)] \quad (20)$$

On the other hand, Mukabi (1995), generated formulae related to the enhancement of strength, deformation resistance (maximum elastic modulus) and linear elastic limit as provided in Equations 22 and 23 and graphically represented in figures 41 to 42, while Figure 26 presents the fundamental concept of stage construction.

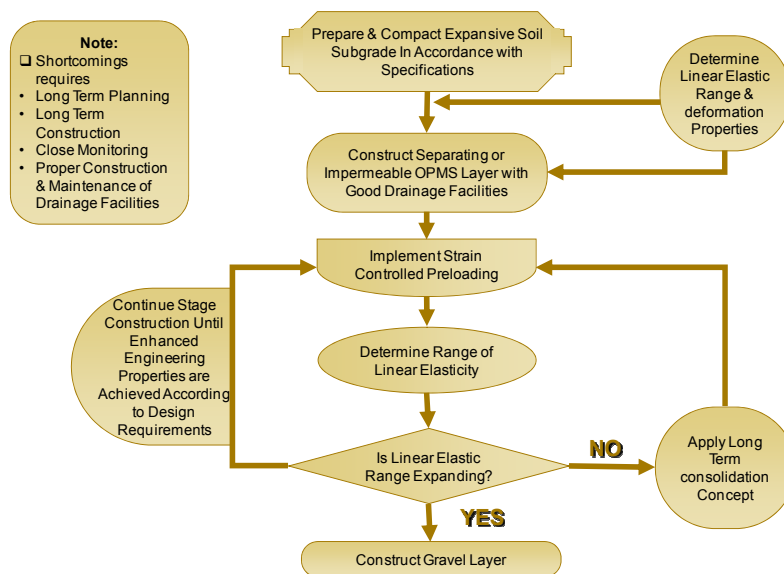


Figure 26 - Fundamental Concept of Long Term Staging Construction

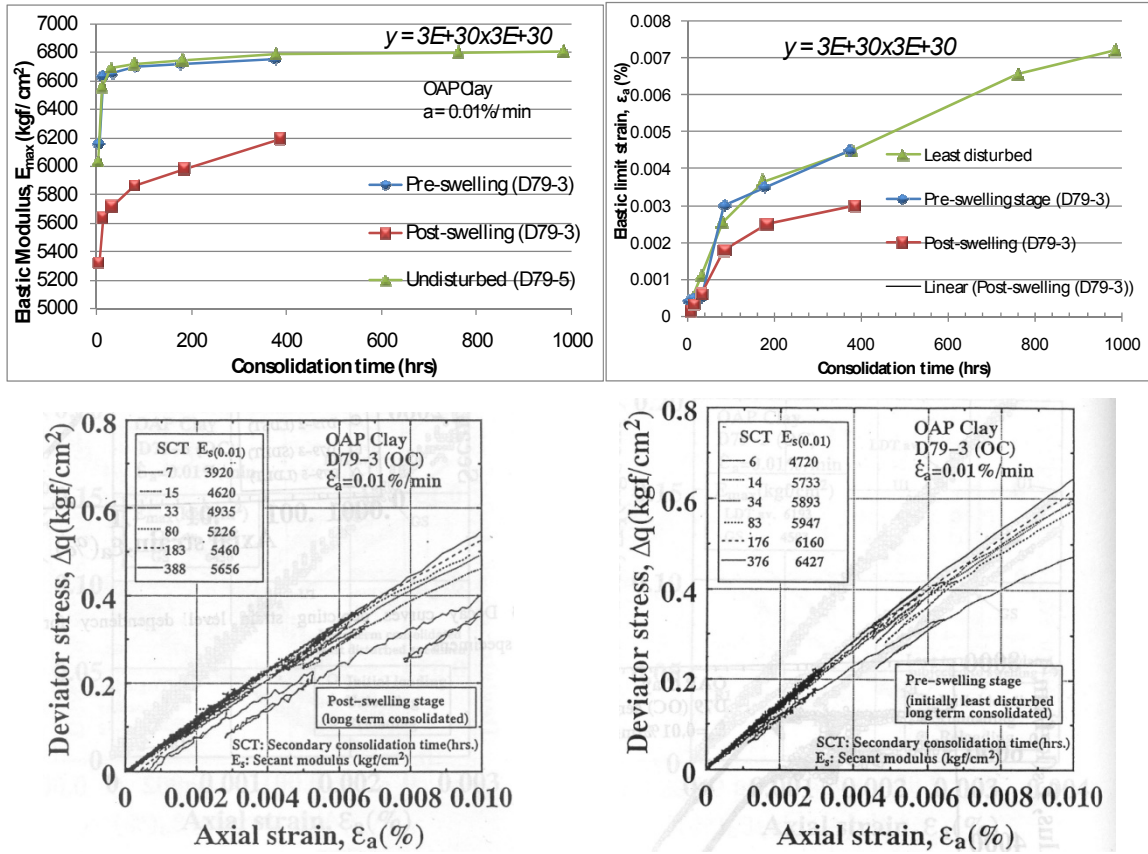


Figure 27 – Consolidation time effect on elastic modulus and deviator stress

#### (5) Effect of Construction Equipment, Vehicular Compaction and Surcharge Pressure

Computation of total and initial settlement resulting from construction and surcharge of upper layers is considered vital since this influences the characteristics of the roadbed soils and the magnitude of their engineering parameters (ref. to Figures 35~36). In computing the total settlement, the generalized Eq. (22) below was adopted.

$$S_T^{ij} = \Delta H_i \frac{C_c^i}{1+e_i} \sum_{j=1}^n \log_{10} \left( \frac{P_0^{ij} + \Delta P_{TC}^k}{P_0^{ij}} \right) \quad (22)$$

where,  $\Delta H_i$  = Thickness of each layer in cm. Back Calculation of induced stresses and strains due to these effects were derived from equations 23 and 24.

$$C_{ci} = \frac{\Delta e_i}{\log_{10} \left[ \frac{(P_0 + \Delta P)}{P_0} \right]} \quad (23)$$

$$\text{Rewriting Equation (7) we obtain,} \quad P_0^{ij} = \frac{\Delta P_{sc}^k}{(10^{\alpha_i} - 1)} \quad (24)$$

Where,  $\alpha_i = \sum_{j=1}^n \frac{\Delta e_j}{C_c^j}$

It is assumed that the stress is induced uniformly and that the magnitude of induced stress reduces proportionally with depth. However, the quantitative reduction is average over the depth of each layer as a logarithmic function of the summed reduction in voids ratio (e)

and compression Index ( $C_c$ ). The stress induced is computed as a resulting value of the post-construction surcharge. This effect is depicted in Figures. 41 and 42 for expansive tropical soils. Figure 43 and the insert equation after Mukabi and Gono (2003a) were used for the design of containing swell for pavement structures constructed within areas of expansive tropical soils.

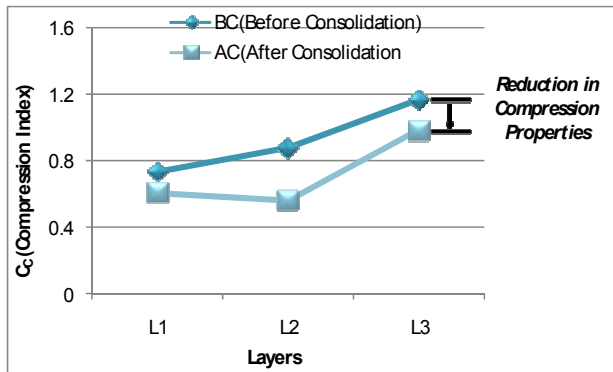


Figure 28 – Reduction in compression

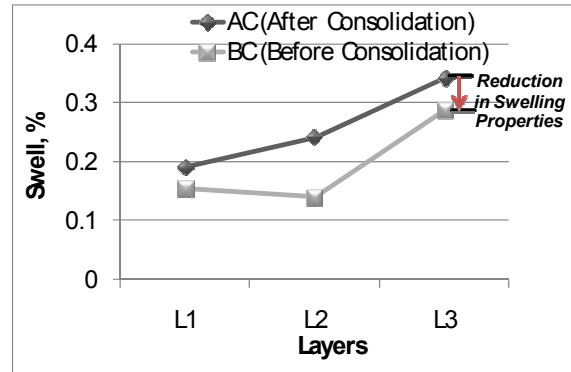


Figure 29 – Reduction in swell

### (6) Dynamic Loading Effects

Subsequent to long-term static loading, the trial sections described by Gono and Mukabi (2003a) were subjected to dynamic loading. As can be noted from Figs. 40 and 41, the three trial sections were initially subjected to around 61 passes of dynamic loading by use of a loaded dump truck of 1.2 axle configuration and front and rear axle loads of 4.5 and 9.5 tons respectively. This vehicle was chosen since it represents the most common type of traffic along the project road (Addis Ababa ~ Goha Tsion).

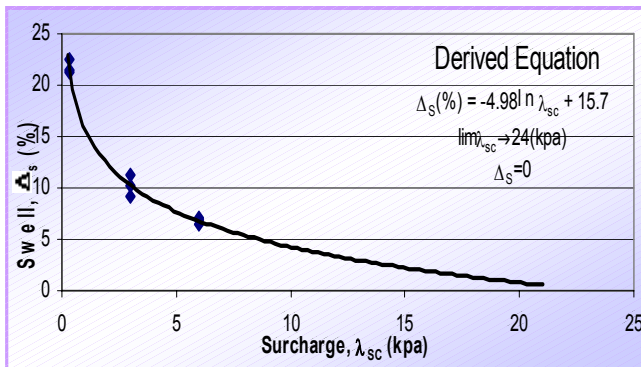


Figure 30 - Surcharge Pressure on Swell

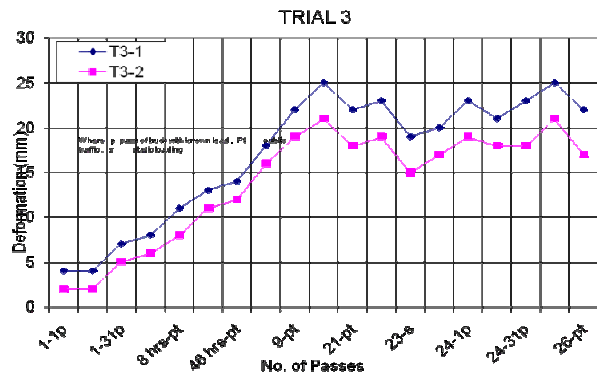


Figure 31 – Deformation characteristics

Deformation during the static loading stages was measured by use of imbedded pegs (ref. to Gono and Mukabi, 2003a), while steel plates were adopted during the dynamic loading stage. In order to analyze the seasonal effects, the sets of both in-situ and laboratory tests were carried out in two stages during the wet and dry seasons under static loading conditions. Dynamic loading was carried out for 20 days subsequent to which the ground response was monitored for 3 days under static loading conditions. Dynamic reloading was then effected for another 4 days after which in-situ measurement of deformation, extrusion of least disturbed samples and material sampling for laboratory testing was undertaken. It can be noted from the results in Fig. 41 that long-term consolidation and

primary dynamic loading tend to enhance the strength and deformation properties of expansive soils.

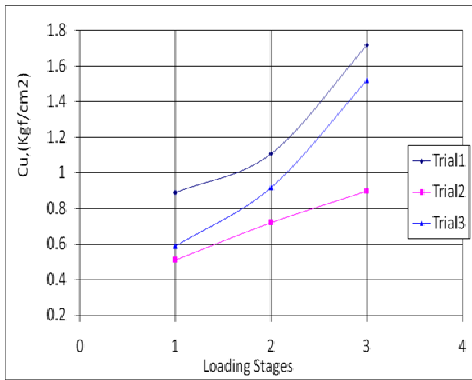


Figure 32 – Static/dynamic loading

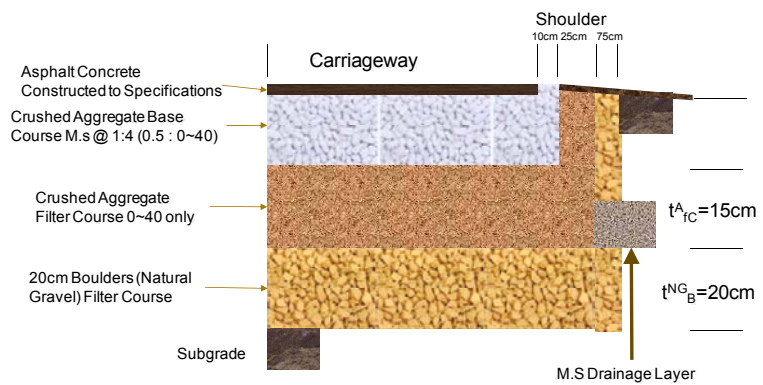


Figure 33 –Coupling design

**Notes:**

1 : Primary Static Loading, 2 : Secondary Static Loading, D : Dynamic Loading

**3.2.7. Coupling Method (Drainage Layer and Suction Stress)**

Figure 46 shows an example of the coupling method that was used in maintenance of some defect areas along the Addis Ababa ~ Goha Tsion Trunk Road in an area that had very high precipitation levels Ethiopia. This method proved quite effective in enhancing the strength, stability, bearing capacity and deformation resistance of the pavement structure under the stated conditions.

**3.2.8. Moisture Control and Interface Technique**

This method, depicted in Figure 47, was also effectively applied in maintaining various sections of road in Ethiopia.

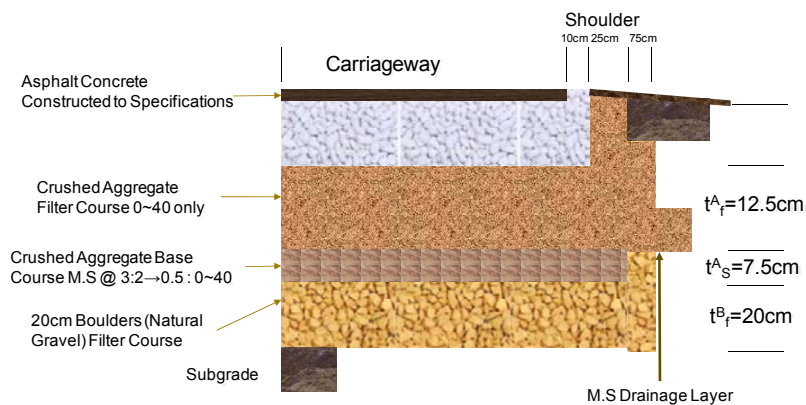


Fig. 34 Depiction of Moisture Control and Interface Technique

**4. MODIFIED ANALYTICAL THEORIES AND CONCEPTS APPLIED IN THE CHARACTERIZATION OF PAVEMENT DESIGN AND CONSTRUCTION**

**4.1.Preamble**

Theoretical considerations are basically made for various factors that influence the response of a pavement structure in correspondence with the measured rebound

deflection. The pre-loading and load intensity effects for example, are considered to be under the repeated dynamic stationary boundary conditions as indicated in Figure 48. Under these conditions, the pavements response to a sequence of moving or Harvesine loads, reflects the intersection between the primary response and the cumulative damage models. However, in this study, the loads are considered to be identical repeated moving loads. In this case the cumulative damage is expressed in terms of the peak primary response to a single moving load and the number of load applications. The load equivalence is considered in terms of the road stress factor introduced by Eisenmann (1975) to account for dynamic loads.

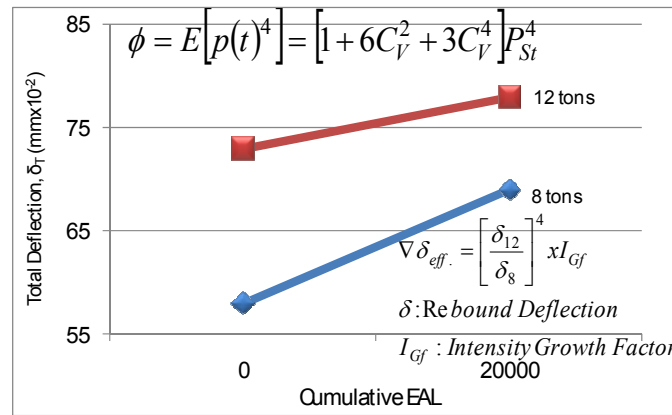


Figure 35 – Pre-loading and load intensity deflection

Under the preceding loading circumstances, the series of deflection basins are characterized by the damped oscillatory motion and energy principles. Since the measurements made are of rebound deflection, an attempt is made to correlate these values and the resilient properties based on linear and equivalent linear analysis of the shear waves propagated through the pavement layers. In carrying out these analysis a newly introduced parameter in the measurement of rebound deflection referred to as “response time” is adopted. This parameter is also applied in deducing quasi-elastic properties of the varying layer materials by applying the theories and principles of seismic wave propagation techniques.

Back analysis of the distressed pavement stress ~ strain and deformation history is made by applying some of the cyclic plasticity models for geomaterials based on non-linear kinematics hardening theory proposed by Yashima et al. (1994). These theoretical considerations are briefly introduced in the subsequently sections.

#### 4.2. Dynamic Loading Effects

Although the equivalency law and hence the fourth power law equations developed at the AASHO road test incorporate actual dynamic load effects based on measurements of the overall loss of serviceability that included dynamic components, attempts to modify these equations have constantly been made. In this study, the equation proposed by Eisenmann (1975) containing a quantifier  $\phi$ , known as the road stress factor, is applied. This equation is adopted because it is considered to be the best mathematical representation of the theory of serial basins introduced in this study. In this relation, it is assumed that dynamic wheel forces are Gaussian, i.e. normal distributions. The value deduced of the fourth power of instantaneous wheel force  $E$  is given by:

$$\phi = E[p(t)^4] = [1 + 6C_V^2 + 3C_V^4] P_{St}^4 \quad (25)$$

where,  $P(t)$  = instantaneous tyre force at time  $t$ ,  $P_{st} = E[p(t)]$  = static (average) tyre force,  $C_v$  = coefficient of varieties of dynamic tyre force and  $E[ ]$  = expectation operator. Eisenmann (1978) further modified Eq. (1) to account for the effects of wheel configuration and tyre pressure in the form of Eq. (26)

$$\phi' = v(\eta_I \eta_{II} P_{st.})^4 \quad (26)$$

where,  $v = 1+6 C_v^2 + 3 C_v^4$  (dynamic road factor),  $\eta_I$  = parameter accounting for wheel configuration for both single or dual tyres and  $\eta_{II}$  = parameter accounting for tyre contact pressures. Intuitively,  $\phi$  and  $\phi'$  are dynamic versions related to the AASHO load equivalent factor (LEF) in the forms:

$$K\phi = vLEF \quad (27)$$

and,  $k\phi' = V(\eta_I \eta_{II})^4 LEF$ ,  $k = (P_{st.})^{-4}$

### 4.3. Transversal Propagation of Stress Induced Waves

In this study, the concept of serial deflection basins is introduced by considering the dynamic wheel load concept. It is assumed that the deflection basins formulated can be mathematically represented by the damping effects of the pavement layers either in a composite or independent form. The damped oscillatory equation of motion is therefore adopted (ref. to Figure 49).

$$\delta_{rd} = c_o e^{ht} \sin\left[(h^2 - \omega_0^2)^{0.5} t + \phi_o\right] \quad (28)$$

where,  $\delta_{rd}$  = rebound deflection,  $C_o$  = constant representing the initial conditions of loading,  $d$  = damping factor of the pavement structure related to layer stiffness,  $t$  = response time measured,  $\omega$  = angular frequency and  $\phi$  = constant representing the initial position and condition of deflection measurement.

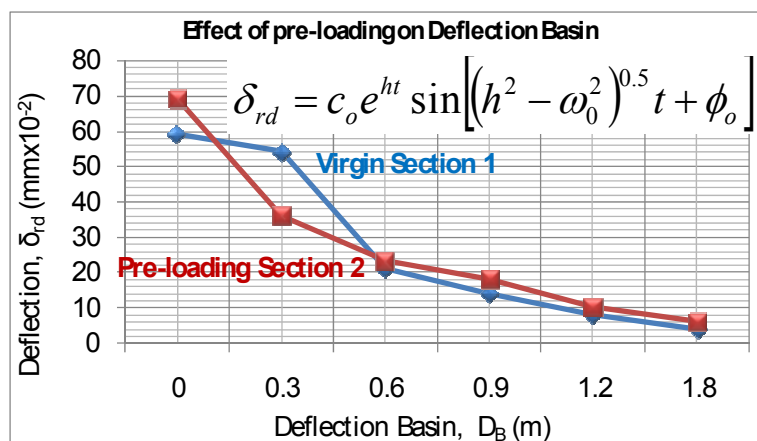


Figure 36 – Deflection basin pre-loading effect

The concept of energy was also applied in analyzing the curvature of the deflection basin in relation to the elastic moduli energy equation, expressed as follows.

$$E(t) = 0.5 C_0^2 e^{-2ht} \left\{ \lambda_a (w_0^2 + h^2) \cos^2 \left[ (w_0^2 + h^2)^{0.5} t + \phi_0 \right] + f_r \sin^2 \left[ (w_0^2 + h^2)^{0.5} t + \phi_0 \right] \right\} \quad (29)$$

where,  $f_r$  is the force constant and  $I_a$ =axle load. It is further considered that the energy decreased exponentially with the increase in time and is expressed as:

$$\frac{dE(t)}{dt} = \frac{d}{dt} \left[ \frac{1}{2} \lambda_a \delta_{rd}^2 + \frac{1}{2} f_r \delta^2 \right] \quad (30)$$

#### 4.4. Theory Of Applying Excitation Truck And Vibration Roller

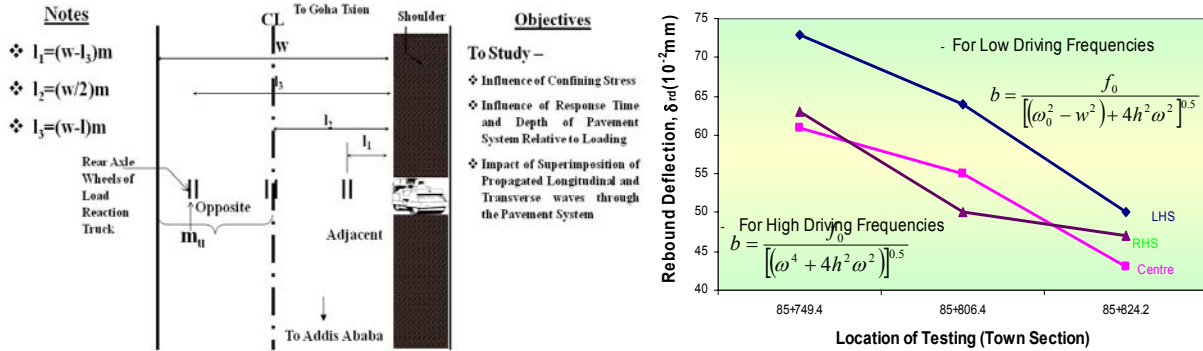


Figure 37 – Rebound deflection measurements and vibration roller effect

Basically, as described in the paper on the “Method of Testing”, the excitation truck and vibration roller were used for purposes of studying the impact and magnitude of disturbance on the quantities of the deflections measured, longitudinal deformation, transversal rebound characteristics and total pavement response. Effects of the variation of the speed of the excitation and vibration modes of the vibration roller are quantitatively analyzed from the following relation of steady state motion, completely specified by an amplitude  $b$  and phase angle  $\psi$ . Figs. 46 (a) and (b) demonstrate this phenomenon.

For low driving frequencies, the phase angle is expressed as:

$$\psi = \arctan \frac{2h\omega}{(\omega_0^2 - \omega^2)} = 0 \quad (31)$$

In this case the driving force and resulting deflection are in phase hence the amplitude is expressed as:

$$b = \frac{f_0}{\left[ (\omega_0^2 - \omega^2) + 4h^2 \omega^2 \right]^{0.5}} \quad (32)$$

For high driving frequencies the amplitude is considered to be

$$b = \frac{f_0}{\left[ (\omega^4 + 4h^2 \omega^2) \right]^{0.5}} \quad (33)$$

In cases whereby  $d$  is small for light damping then:

$$b = \frac{f_0}{\omega^2} \quad (34)$$

The phase angle is then given by

$$\psi = \arctan \frac{2hw}{(\omega_0^2 - \omega^2)} = \pi \quad (35)$$

In such a case as the frequency of  $\omega$  of the impressed force is increased, the amplitude decreases and the phase angle tends towards  $\pi$

#### 4.5. Shear Wave Propagation Through Pavement Layers

The analysis of the shear wave propagation through pavement layers is schematically represented in Figure.38. It was carried out by applying the concepts related to the Linear (LIN) and Equivalent Linear (EQL) methods. These methods of analysis are commonly made by multiple reflection of vertically propagating horizontal components of shear waves through multiple layered profile one dimensional system Assuming the deflection at any layer n is given by:

$$\delta_{rd} = \delta_{rd}(Z_1 t) = \Delta_{rd}(Z) e^{i\omega t} \quad (36)$$

where,  $\Delta_{rd}$  is the total displacement .The equation of motion is then given by:

$$\rho_n \frac{\partial^2 \delta_{rd}^n}{\partial t^2} = G_n \frac{\partial^2 \delta_n}{\partial Z^2} + \eta_n \frac{\partial^3 \delta_n}{\partial Z^2 \partial t} \quad (37)$$

where,  $\omega \eta_n = 2G_n h_n$ ,  $\rho$  = density of pavement layer,  $G$  = shear modulus and  $h$  is damping.

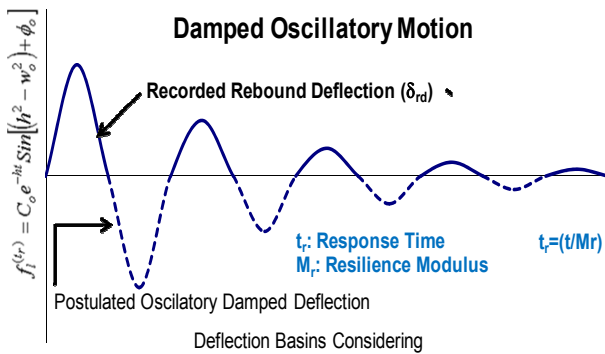


Figure 38 – rebound deflection

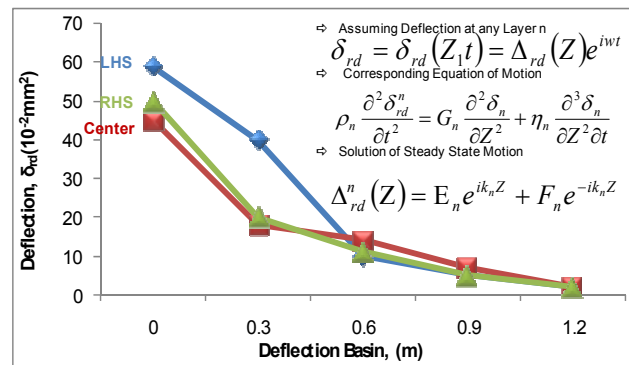


Figure 39 – Deflection basin

The solution of the resulting differential equation for the steady state harmonic motion is obtained as follows:

$$\delta_{rd}^n (Z) = E_n e^{ik_n Z} + F_n e^{-ik_n Z}$$